Insights into the influence of solvent polarity on the crystallization of poly(ethylene oxide) spin-coated thin films via *in situ* grazing incidence wide angle x-ray scattering.

Daniel T. W. Toolan,[1] Anna Isakova,[2] Richard Hodgkinson,[1] Nik Reeves-McLaren,[3] Oliver S. Hammond,[4] Karen J. Edler,[4] Wuge H. Briscoe,[5] Thomas Arnold,[6] Tim Gough,[7] Paul D. Topham,[8] and Jonathan R. Howse.[1*]

1. Department of Chemical and Biological Engineering, University of Sheffield, Sheffield. S1 3JD. UK
2. Chemical Engineering and Applied Chemistry, Aston University, Birmingham, B4 7ET, UK
3. Department of Materials Science and Engineering, University of Sheffield, Sheffield. S1 3JD. UK
4. Department of Chemistry, University of Bath, Claverton Down, Bath, BA2 7AY, UK
5. School of Chemistry, University of Bristol, Cantock's Close, Bristol, BS8 1TS, United Kingdom
6. I07 Beamline, Harwell Science and Innovation Campus, Diamond Light Source Ltd., Didcot OX11 0DE, U.K.
7. School of Engineering and Informatics, University of Bradford, Bradford, BD7 1DP, UK
8. Aston Materials Centre, Aston University, Birmingham, B4 7ET, UK.

Abstract

Controlling polymer thin-film morphology and crystallinity is crucial for a wide range of applications, particularly in thin-film organic electronic devices. In this work, the crystallization behavior of a model polymer, poly(ethylene oxide) (PEO), during spin-coating is studied. PEO films were spun-cast from solvents possessing different polarities (chloroform, THF and methanol) and probed via *in situ* grazing incidence wide angle x-ray scattering. The crystallization behavior was found to follow the solvent polarity order (where chloroform < THF < methanol) rather than the solubility order (where THF > chloroform > methanol). When spun-cast from non-polar chloroform, crystallization largely followed Avrami kinetics, resulting in the formation of morphologies comprising large spherulites. PEO solutions cast from more polar solvents (THF and methanol) do not form well-defined highly crystalline morphologies and are largely amorphous with the presence of small crystalline regions. The difference in morphological development of PEO spun-cast from polar solvents is attributed to clustering phenomena that inhibit polymer crystallization. This work highlights the importance of considering individual components of polymer solubility, rather than simple total solubility, when designing processing routes for the generation of morphologies with optimum crystallinities or morphologies.

Introduction

Poly(ethylene oxide) (PEO) is a semicrystalline polymer that exhibits complex solution behavior owing to the interplay of hydrophilic and hydrophobic sites along the polymer chain. PEO finds a wealth of applications in the biomedical and energy fields,[1] in addition to numerous industrial applications, such as adhesives,[6] detergents,[7] inks,[8] lubricants[9] and textiles. As with all materials research there is strong link between the structure formed by the materials during processing and final material or device performance. PEO has therefore been the subject of intense

research interest with regards to both its crystallization behavior and its rich and complex solution behavior.

Numerous studies have focused on understanding the crystallization of PEO from the melt in both bulk and thin-film systems, utilizing techniques such as x-ray scattering,[2] atomic force microscopy,[3] optical microscopy[4] and FT-IR spectroscopy.[5]

Polymer thin-films, however, are often produced *via* solution processing methods such as spin-coating, where a polymer solution is deposited on a substrate that is rotated at high speed (typically between 1,000 & 10,000 rpm), resulting in the formation of a thin polymer film in a matter of seconds. There then exists a trade-off between the ideal physical processing steps required to produce a film of the required thickness and the structure and morphology of the film itself. Film thinning is often simplified as a two stage process, where initially, hydrodynamic thinning takes place due to the centrifugal force acting on the solution, which is then proceeded by film thinning dominated by solvent evaporation.[6] Hydrodynamic thinning is dependent upon the solution viscosity, radial speed and acceleration,[6b, 7] whilst, evaporative thinning is dependent upon the vapor pressure of the solvent.[6a, 8]

As solvent is rapidly removed *via* evaporation, a fine balance of complex self-assembly processes take place, such as phase-separation,[9] crystallization,[10] stratification,[11] and agglomeration, resulting in the formation of highly complex and intricate morphologies. For shallow quenches (when solvent is lost slowly), the morphology will evolve towards thermodynamic equilibrium, whilst for deep quenches (when solvent is removed rapidly), the morphology may become frozen far from thermodynamic equilibrium or evolve down kinetic pathways. As such, through solution processing, a large range of morphologies are accessible from a relatively straightforward processing route.

When PEO is solution cast, it typically crystallizes with a monoclinic unit cell containing four 7_2 helices, which form chain folded lamellae that often organize into

spherulites.[12] The hierarchical crystalline structure of PEO is shown schematically in Figure 1.

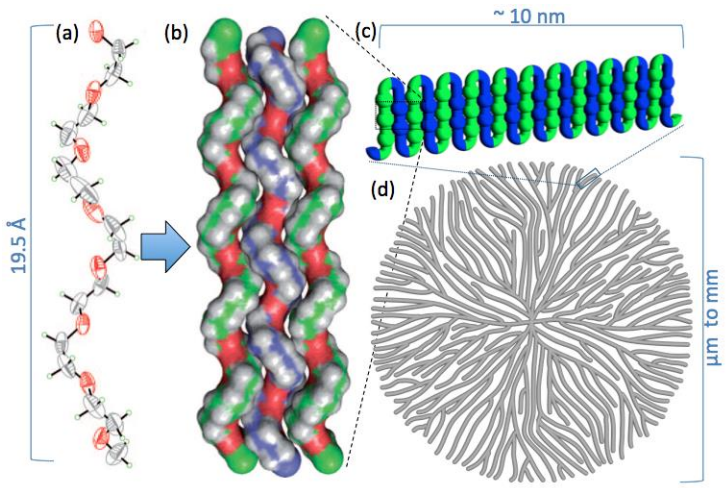

Figure 1: Typical hierarchical crystal structure of PEO, from individual chain conformation, packing and folding to spherulite. a) and b) have been taken and adapted from reference 13.

PEO has been found to exhibit sophisticated solution behavior, forming clusters (aggregates) in aqueous media and in other polar solvents, such as methanol.[14] The origin of clustering has been the subject of intensive research efforts and is not fully understood, but could be due to: polymer crystallization, inter-chain physical cross-links, hydrogen bonding or chain end effects.[14a, 14d, 14f, 15] How the solution behavior of PEO may influence crystallization during thin-film processing is an area that has not yet been fully explored.

Due to the numerous applications of polymer thin-films produced *via* solution processing, understanding how crystallization in thin solvent-rich films differs from crystallization from the melt is of both fundamental and commercial importance. Further significance arises from the field of organic electronics, where the crystallinity of the solvent-cast film plays a crucial part in determining device performance.[16] Due to the rapid, non-equilibrium nature of the spin-coating process, we still do not fully understand the intricacies of crystallization occurring during processing and so are unable to rationally design processing strategies that yield

materials with optimum crystallinities. Driven by the pursuit of increasing OPV device efficiencies, the majority of experimental studies have focused on understanding the crystallization of semiconducting polymers with solubilized fullerene derivatives. Such systems are directly applicable to applications in organic electronics but are highly complex due to the poor solubility of many semiconductor polymers in organic solvents and the combination of a polymer with a small molecule (itself with intricate aggregating and dimerizing behavior).[17] In the work herein, the well-studied, semi-crystalline PEO is used as a model polymer system to further the understanding of how solvent properties influence crystallization occurring during spin-coating.

A wide range of *in situ* experimental techniques have been developed to study processes that occurs during the spin-coating of polymers based upon microscopy, and laser/x-ray scattering,[18] which have revealed information regarding phase separation,[19] self-stratification[11b, 11d] and crystallization.[17, 20] Recent, *in situ* microscopy studies have shown that polymer concentration and spin-coating process parameters (rotation speed and acceleration) affect both the crystallization kinetics of PEO. [20] Herein, we investigate how the complex solution behavior of PEO interplays with the rapid crystallization that occurs during spin-coating, by exploiting *in situ* grazing incidence wide angle x-ray scattering (GIWAXS). Through this approach we are able to identify the crystallization pathway (e.g. emergence of crystalline phases along with any intermediate phases) and obtain information regarding crystallization kinetics.

PEO is highly soluble in a wide range of organic solvents, such as chloroform, methanol and tetrahydrofuran (THF), which are interesting to study because they possess different polarities and solubilities, whilst having largely similar vapor pressures. As such, the drying kinetics, and hence the quench through the phase diagram, are likely to be highly similar and are unlikely to affect the crystallization process. Hansen solubility parameters give an indication of the solubility of a material in a specific solvent. The total solubility, δ_t, is divided into three parameters, δ_d, δ_p

and δ_h, which represent the contribution of dispersion forces, polar interactions and hydrogen bonding (H-bonding), respectively. The Hansen solubility parameters of THF, chloroform and methanol are given in Table 1.[22] Özdemir and Güner showed that the solvency power of the selected solvents for PEO decreases in the order: THF > chloroform > methanol,[23] whilst the polarity of solvents increases as: chloroform > THF > methanol.

Through studying in detail the evolution of crystal structures of PEO when cast from chloroform, THF and methanol, this work provides insight into how both the overall solubility and polarity affect PEO crystallization. Put simply, if solubility dominates, the nature of PEO crystallinity should be determined by the solubility order, whereas if polar interactions dominate, PEO crystallinity will be dictated by the polarity order.

Table 1: Dielectric constants and Hansen solubility parameters of solvents studied.[22]

Solvent	Vapour pressure / mm Hg (20 °C)	Hansen solubility parameters ($MPa^{1/2}$) at 25°C				Dielectric constant
		δ_d (dispersion)	δ_p (polar)	δ_h (H-bond)	δ_t (total)	
THF	143	16.8	5.7	8.0	19.4	7.56
Chloroform	160	17.8	3.1	5.7	19.0	4.81
Methanol	98	15.1	12.3	22.3	29.7	32.7

Experimental

Poly(ethylene oxide) (PEO) (M_n = 4 kDa, 10 kDa and 34 kDa) (Aldrich), used as supplied, was dissolved in either chloroform, methanol or tetrahydrofuran (THF)

(Aldrich) at 10 wt% by stirring continuously for 12 hours. For clarity, the chemical structures are presented in Figure 2.

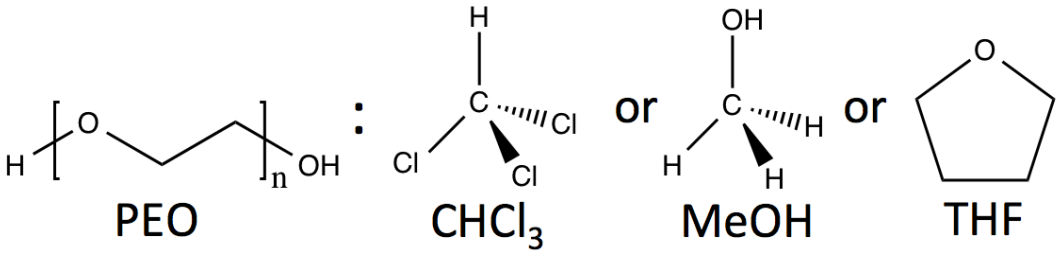

Figure 2: Chemical structures of systems studied in this work: PEO (10 wt%) in either chloroform ($CHCl_3$), methanol (MeOH) or tetrahydrofuran (THF).

Time resolved grazing incidence wide-angle x-ray scattering (GIWAXS) was performed at I07 (Diamond Light Source, Rutherford, UK) using a Pilatus 2M 1475 x 1679 pixel detector. The *q* max of the detector was determined as q_x = 6.35 $Å^{-1}$ and q_y = 7.23 $Å^{-1}$ using a silver behenate standard. The spin-coater comprised of a brushless DC motor [Premotech, BL48 EB (4 wire)] fitted with an aluminum chuck (20 mm diameter) on top of which circular glass substrates were placed (Fisher Scientific, used as received). Approximately 200 μl of polymer solution was deposited *via* a syringe pump with a needle placed above the center of the circular substrate.

The *in situ* x-ray scattering procedure is shown schematically in Figure 3. Data were collected at a rate of 20 fps for; (i) the glass substrate, denoted as time, t = -60 to -30 s (background); (ii) deposition of polymer solution, t = -30 to 0 s (solution scattering in a grazing geometry); (iii) substrate acceleration to 1500 rpm at t = 0 to 3 s; (iv) film formation dynamics at t = 3 to 63 s; (v) substrate deceleration from 1500 to 0 rpm at t = 63 to 66 s; and (vi) the final cast film at t = 66 to 126 s.

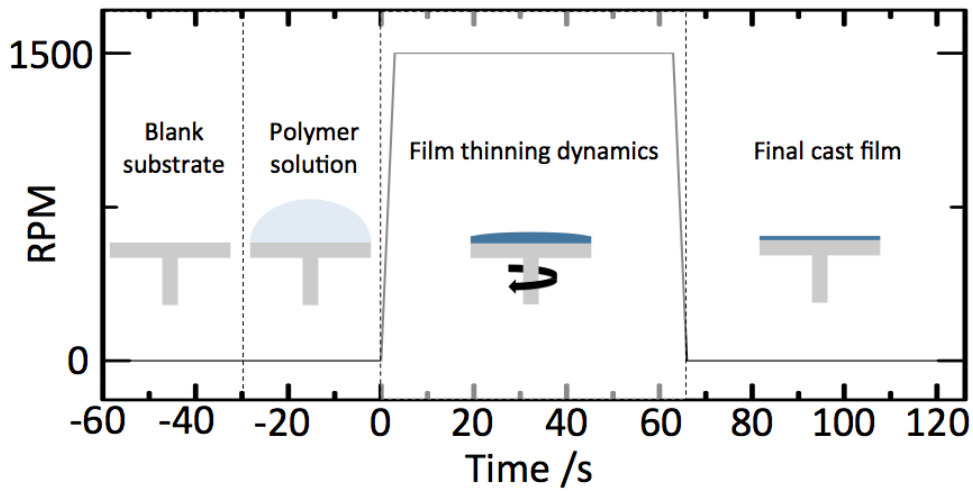

Figure 3: Schematic of data collection process. Time = 0 is defined as the instance the motor begins to turn.

Results

Crystallization in thin polymer films is determined by both the properties of the polymer (e.g. chemistry, architecture, molecular weight) and the processing route (e.g. solvent, substrate, spin speed, temperature, evaporation rate). Figure 4 presents optical microscopy images taken using crossed polarizers and shows a range of crystalline morphologies that form when PEO of varying molecular masses (M_n = 4 kDa, 10 kDa and 34 kDa) was spun-cast from; chloroform, THF or methanol. When spun-cast from chloroform, the final films are highly crystalline with morphologies consisting of large well-defined spherulites, with the spherulite size decreasing with increasing molecular weight.[24] Conversely, when low molecular weight PEO was spun-cast from THF or methanol, the morphology was predominantly amorphous with some small crystalline regions. For PEO spun-cast from either THF or methanol, the crossed polarized optical microscopy images show that as the PEO molecular weight increased, the size of the crystalline regions also increased, however, well-defined spherulite crystalline domains were not formed.

Clearly, solvent plays an important role in determining how PEO crystallizes and thus drives the final morphology that is obtained. Interestingly, the crystallization behavior of PEO does not simply follow the solubility order (where THF > chloroform > methanol), as might be expected and is thus the motivation behind this study.

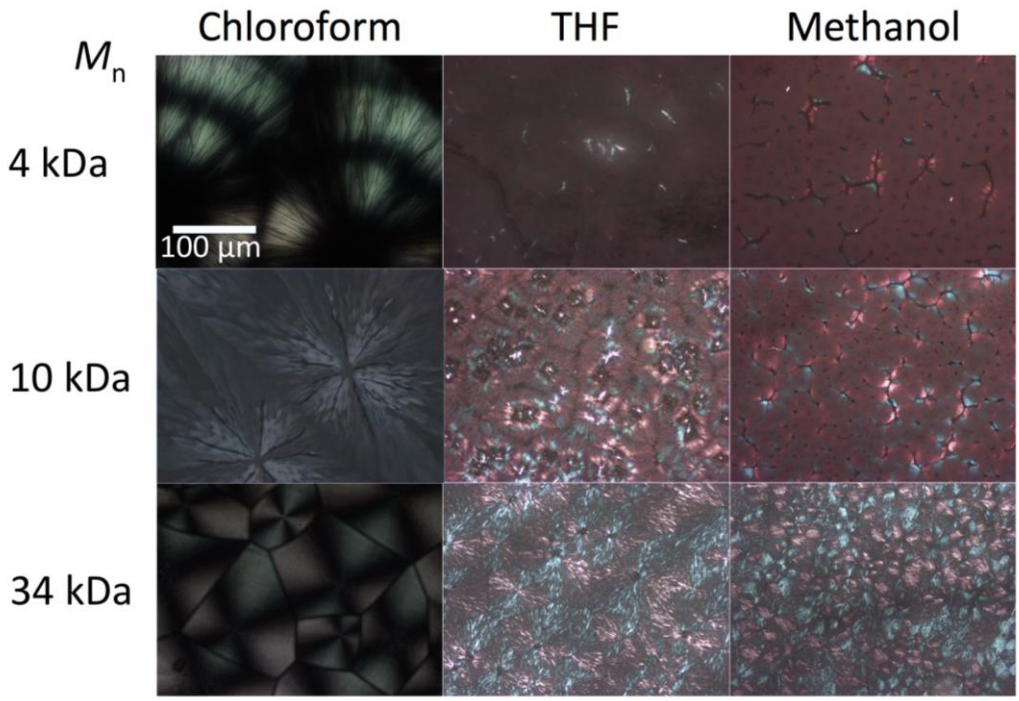

Figure 4: Optical micrographs taken using crossed polarizers of PEO (M_n = 4 kDa, 10 kDa, 34 kDa) spun-cast from either chloroform, THF or methanol at 1500 rpm.

In order to further investigate the effect of solvent on polymer crystallization that occurs upon processing, *in situ* GIWAXS was performed during the spin-coating of PEO from different solvents (chloroform, THF & methanol). Figure 5 presents radially averaged x-ray scattering data as a function of time for PEO of different molecular masses spun-cast from 10 wt% chloroform solution, which correspond to the left column of final crystalline morphologies shown in Figure 4.[a]

[a] Radially-averaged scattering data is presented as a colour-mapped intensity chart in Supplementary Figure S1.

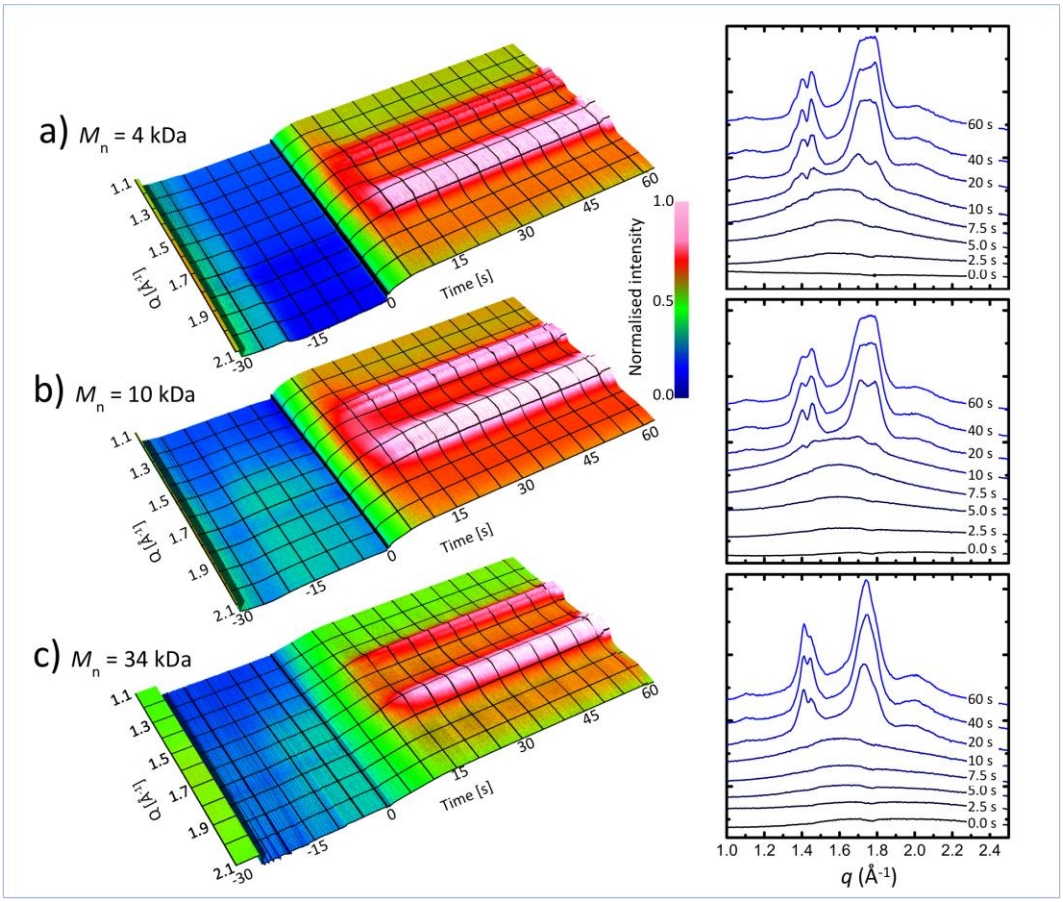

Figure 5: *In situ* grazing incidence scattering data showing the development of crystallinity for PEO (M_n = 4 kDa, 10 kDa and 34 kDa) films spun-cast from 10 wt% chloroform solutions at 1,500 rpm. a-c) Radially integrated scattering data as a function of time with corresponding cross sections at between 0 and 60 s, for 4 kDa (a), 10 kDa (b) and 34 kDa (c) PEO.

The radially integrated x-ray scattering data presented in Figure 5a-c gives an overview of how the scattered x-ray signal changes with respect to both film formation dynamics and the crystallization of PEO of different molecular weights spun-cast from chloroform solutions.

From these data, several distinct stages can be identified:

i) -30 to -25 s: the polymer solution is deposited onto the substrate surface, resulting in a sharp decrease in the scattered intensity, as the beam is now passing through the thick polymer solution 'droplet'.

ii) 0 to ~5 s: the polymer film thins due to a combination of hydrodynamic and evaporative thinning, the scattered intensity increases accordingly and additionally a broad scattering feature (with a maximum at q = ~1.59 Å^{-1}) emerges at 2.5, 2.55 and 2.95 s for 4 kDa, 10 kDa and 34 kDa PEO, respectively. This broad scattering feature is indicative of a pre-ordering stage, prior to crystallization.

iii) ~5 to ~7: the intensity of this broad scattering feature proceeds to increase until the onset of two distinct scattering peaks (q = ~1.42 and 1.73 Å^{-1}) at 6.85, 9.15 and 11.35 s, for 4 kDa, 10 kDa and 34 kDa PEO, respectively.[b] The scattering peaks at 1.42 and 1.73 Å^{-1} are identified as the 120 and 032 reflections and are indicative of PEO crystallization.[2, 12]

iv) ~7 to 60 s: the intensity of the 120 and 032 reflections increases as crystallization proceeds.

The radially averaged data profiles (Figure 5a-c, right) show that for all of the PEO molecular masses studied here, the 120 crystalline reflection is split, with two maxima at q = 1.37 and 1.44 Å^{-1}, and that for 4 kDa and 10 kDa PEO, the 032 reflection shows significant broadening between q = 1.71 and 1.79 Å^{-1}. This peak splitting/broadening is ascribed to a consequence of both the grazing incidence geometry giving rise to reflections of the incident beam from both top and bottom faces of the glass substrate and the large size of the PEO spherulites.

The development of the 032 reflection as a function of time is shown in Figure 6a and is related to the relative degree of crystallinity in the system. These data show that upon substrate acceleration to 1,500 rpm, the intensity of the 032 reflection rapidly increases due to crystallization of the PEO (owing to a rapidly increasing

[b] Onset times for the emergence of crystalline 120 and 032 reflections were determined through observation of the first frame in the kinetic data set, where distinct peaks at q = ~1.42 and 1.73 Å^{-1} are discernable from the initial broad scattering feature.

polymer concentration as the solvent evaporates). The crystallization process appears to take place in two stages; an initial rapid crystallization, followed by a slightly slower growth step. Such two-stage crystallization has previously been observed for doctor bladed P3HT:PCBM thin-films.[25] The rate and duration of crystallization are seen to decrease and take longer with increasing molecular weight, due to decreased mobility of the polymer chains and hence the longer rearrangement times. The normalized intensity data for the 34 kDa PEO system exhibit large-scale fluctuations between 20 and 60 s. Such oscillations are ascribed to constructive interference between the motor rotation speed, the camera frame rate and motor precession. At 65 s the intensity of the intensity of the 032 reflection shifts as the substrate decelerates and the substrate stops spinning, which removes any time averaging effects brought about by any precision of the rapidly rotating substrate.

The kinetics of PEO crystallization can be explored further using the Avrami model, commonly used to describe the kinetics of the transformation of phases under isothermal conditions and is given in Equation 1:[26]

$$\emptyset_c = 1 - e^{-zt^n} \qquad \text{(Eq.1)}$$

where $\emptyset_c$ is the crystallinity in the crystallizable material at time *t*, *z* is a constant dependent upon nucleation and growth rate and *n* is related to the type of nucleation and growth geometry.

Although the spin-coating process is not strictly isothermal,[27] the Avrami equation offers an initial framework for understanding the underlying crystallization mechanisms. The normalized apparent degree of crystallinity as a function of time is shown in Figure 6b for PEO with M_n = 4 kDa (black line), 10 kDa (red line) and 34 kDa (blue line), spun-cast from 10 wt% chloroform solution at 1,500 rpm, where the

apparent degree of crystallinity is defined as the ratio of the area under the 120 and 032 reflections to the total scattering area.[28] The data does not exhibit a stereotypical "s" shaped curve commensurate with Avrami processes. However, good Avrami fits (Figure 6b magenta lines, with associated fitting parameters given in Table 2) were obtained when the data were modeled between 9 to 13, 10 to 17, and 11 to 19.5 s, for PEO with M_n = 4 kDa, 10 kDa & 34 kDa, respectively, with Avrami exponent *n* around three, consistent with spherulitic crystallization from heterogeneous nuclei. The Avrami rate constant, *z*, decreased with increasing molecular weight, as expected, due to decreasing polymer mobilities. This data show that when PEO is spun-cast from chloroform, the majority of the crystallization from solution is consistent with theory. However, during both the early and late stages of crystallization, the data do not fit the Avrami equation. This could be due to crystallization being coupled with other transitions competing with crystallization, such as gelation, late on in the spin-coating process, leading to rapidly increasing viscosities that significantly reduce polymer mobility and the early emergence of a pre-ordering structure (q = ~1.59 $Å^{-1}$).

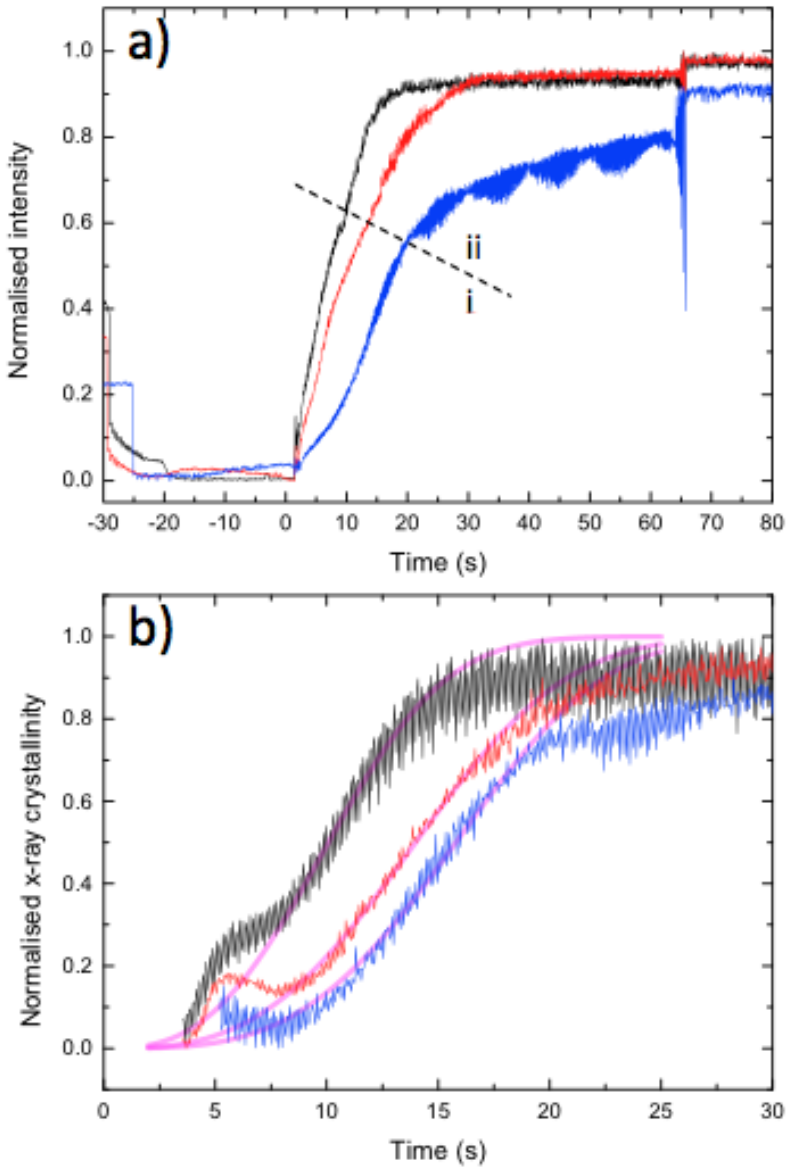

Figure 6: a) Normalized intensity of the 032 peak as a function of time and b) normalized crystallinity of PEO M_n = 4 kDa (black line), M_n = 10 kDa (red line) & M_n = 34 kDa (blue line) spun-cast from chloroform, with respective Avrami fits (magenta lines).

Table 2: Avrami parameters *n* and *z* corresponding to fits of the normalized crystalinity of PEO spun-cast from chloroform.

	n	*z*
PEO M_n = 4 kDa	2.81	0.087

PEO M_n = 10 kDa	3.02	0.063
PEO M_n = 34 kDa	3.32	0.057

So far, data have been presented for the spin-coating of PEO of various molecular weights from chloroform, which shows that crystallization from a non-polar solvent occurs in a highly similar manner to that from the melt, where the process may be largely described *via* Avrami kinetics and large well-ordered spherulites form. However, the polymer-solvent interactions are pivotal in controlling this kinetic process, and thus can direct the final morphology obtained. To study the effect of solvent polarity on crystallization, PEO was spun-cast from solvents with increasing polarity (with respect to chloroform): THF and methanol. The radially averaged scattering data are presented in Figure 7 & 8, respectively.

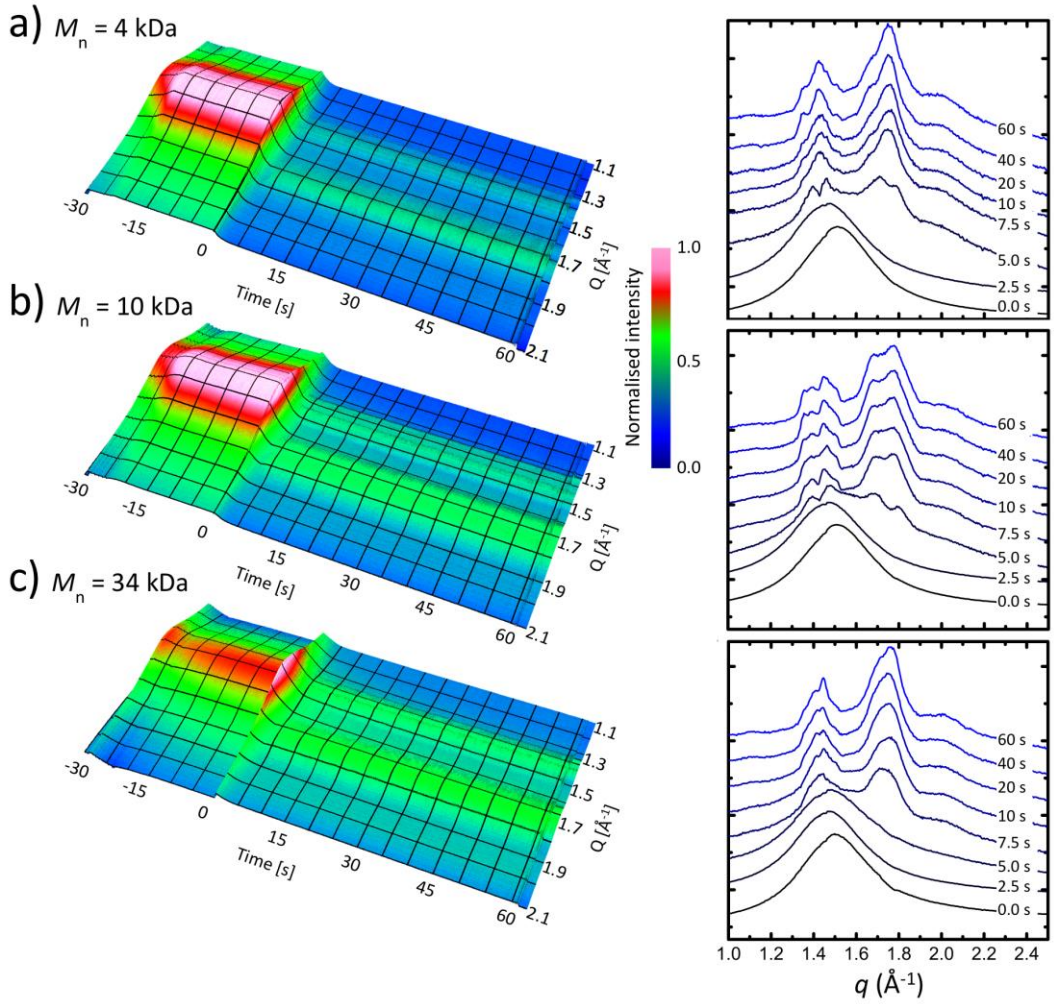

Figure 7: *In situ* grazing incidence scattering data showing the development of crystallinity for PEO (M_n = 4 kDa, 10 kDa and 34 kDa) spuncast from 10 wt% THF solutions at 1,500 rpm. a-c) Radially integrated scattering data as a function of time with corresponding cross sections at between 0 and 60 s, for 4 kDa (a), 10 kDa (b) and 34 kDa (c) PEO.

For the PEO films spun-cast from THF (Figure 7 a-c), the data show that upon deposition of the polymer solution prior to spin-coating there is an intense broad scattering feature at q = 1.49 Å^{-1}, which is of a consequence of scattering from the pure solvent (scattering data for pure solvents is presented in Supplementary Figure S2). When the PEO solutions are subsequently spun-cast, the solvent scattering feature rapidly decays as solvent is lost from the system and the 120 and 032 reflections emerge as PEO crystallization occurs.

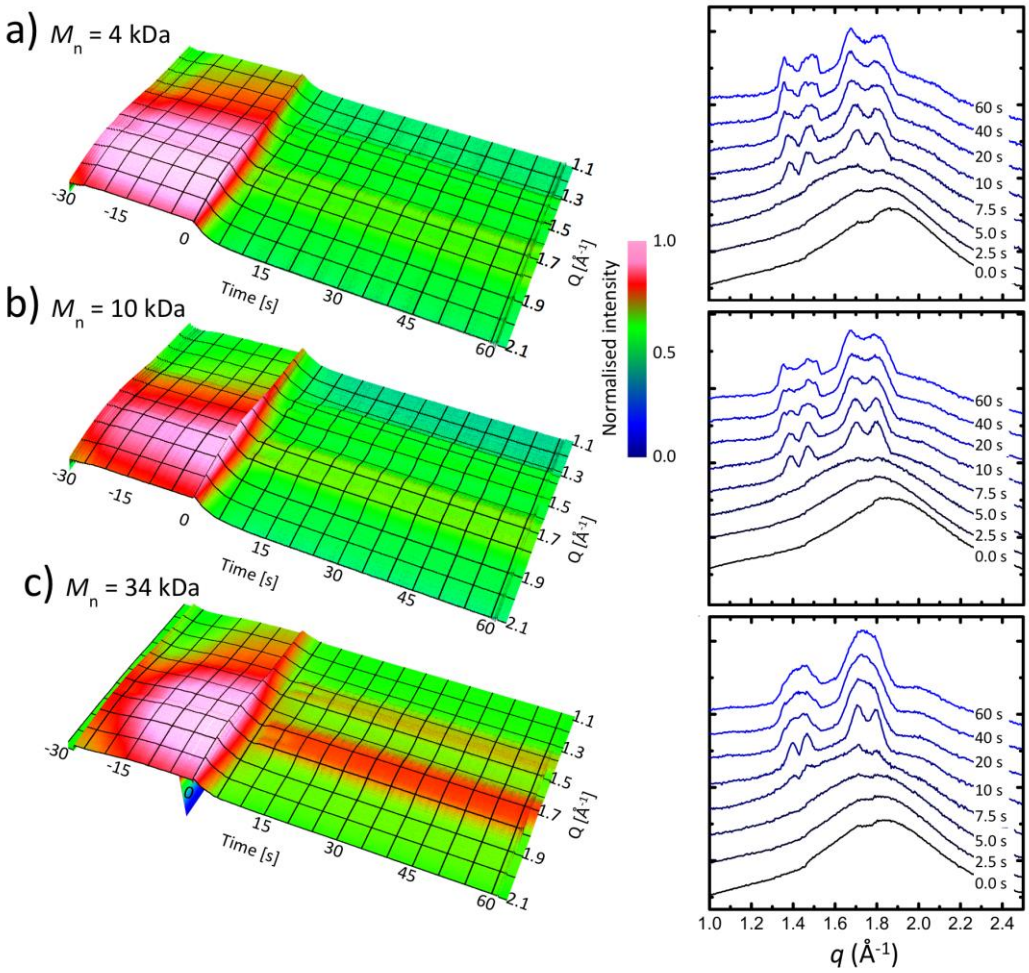

Figure 8: *In situ* grazing incidence scattering data showing the development of crystallinity for PEO (M_n = 4 kDa, 10 kDa and 34 kDa) films spun-cust from 10 wt% methanol solutions at 1500 rpm. a-c) Radially integrated scattering data as a function of time with corresponding cross sections at between 0 and 60 s, for 4 kDa (a), 10 kDa (b) and 34 kDa (c) PEO.

The PEO films spun-cast from methanol solutions (Figure 8a-c) show an initial solvent scattering feature prior to spin-coating [as observed for PEO THF solutions, but at higher q (~1.8 Å^{-1}) that decays once spin-coating begins]. The highest molecular mass PEO spun-cast from methanol (M_n = 34 kDa, Figure 8c) exhibits the development of pronounced 120 and 032 reflections as observed when PEO was

spun-cast from chloroform and THF, whilst for the lower molecular weight PEO spun-cast from methanol (M_n = 4 kDa and 10 kDa, Figure 8a and b, respectively), the 120 and 032 reflections are significantly weaker. The scattering data show that only the high molecular weight PEO (M_n = 34 kDa) exhibits a significant degree of crystallinity, whilst the lower molecular weight PEO films (M_n = 4 kDa and 10 kDa) only exhibit a low degree crystallinity, in agreement with the crossed polarized microscopy images shown in Figure 4.

The *in situ* scattering data show that when PEO was processed from both THF and methanol, scattering from the solvent dominates the early stages of the spin-coating process and once the majority of solvent is removed, PEO crystalline features are observed. Interestingly, when PEO was spun-cast from chloroform no initial solvent scattering features were observed. As chloroform is the most electron dense of the solvents studied, it would be expected to show the strongest solution scattering features. The PEO chloroform solutions do not exhibit features commensurate with solution scattering, as-such, PEO must be well solubilized by the chloroform leading to a high proportion of solvent-monomer interactions. Comparatively, THF and methanol PEO solutions exhibit strong solution scattering features, indicating a high proportion of solvent-solvent interactions, within these systems.

When PEO was processed from a non-polar solvent (chloroform), polymer crystallization proceeds via the formation of large, highly ordered spherulites, which correlate well with Avrami kinetics. When the solvent polarity was increased the final morphologies of the PEO films are largely amorphous containing small crystalline regions.

It is well reported that PEO forms clusters in polar solvents,[14a, 14c, 14d] where inter- and intramolecular dipole-dipole interactions result in clustering and has been extensively studied using Small Angle Neutron Scattering (SANS).[14d] Clearly, such interactions have a dramatic affect on the morphological development and

crystallization behavior of PEO. This is attributed to the fact that clustering reduces the propensity of PEO to form highly ordered crystalline structures through increasing the kinetic barrier for polymer chain straightening, required for packing to form chain folded lamellae that organize into higher order structures.

To further test our hypothesis, the role of solvent interactions on PEO crystallization was extended to include two further non-polar solvents, toluene and dichloromethane. The findings are provided in the Supporting Information, including microscopy images taken under crossed polarizers (Supplementary Figure S3). In short, as predicted from our discoveries discussed herein, toluene and dichloromethane do not appear to induce clustering and therefore produce films comprising well-defined spherulitic structures. Importantly, all of the solvents selected in our study are considered to be 'good' solvents for PEO, however, our work herein clearly reveals that importance should be placed on individual solvent contributions, such as polarity, rather than overall solubility.

Conclusions

This work has provided new insight into how PEO crystallizes from solution during spin-coating and the important role that solvent plays in controlling the crystallization process. When PEO was spun-cast from non-polar solvents, crystallization was observed to occur in a similar manor to that of crystallization from the melt. When the solvent polarity was increased, the ability of PEO to form highly ordered crystalline morphologies was inhibited. We attribute this to be a consequence of PEO forming cluster-type structures that increase the barrier to chain-straightening required for the formation of aligned, chain-folded lamellae. It is therefore important to note that while a molecule as a whole may dissolve well, clustering can occur when the subunits of a molecule tend to demix. As such, we find that the degree of crystallinity for solution-processed PEO does not follow the solubility order: THF > chloroform > methanol, but instead follows the polarity order: chloroform > THF, methanol. Such studies, as shown here, show the complex interplay between processing

conditions, molecular mass, and solubility. It further shows how understanding of the individual components contributing to polymer solubility has a pronounced effect on the final morphology and crystallinity of the final processed film. Given the strong correlation between crystallinity and conductivity/mobility in polymer electronic devices, our work herein highlights that when designing processing routes, greater consideration of the disparate solvent parameters, beyond the total solubility of the polymer solute, is critical in order to achieve optimum thin-film properties.

Acknowledgements

Thanks to Diamond Light Source and European Synchrotron Radiation Facility for providing beam time under allocations SI328-1 and MA 1316, respectively. Some parts of the research leading to these results has received funding from the European Union Seventh Framework Programme (FP7/2011 under grant agreement ESTABLIS no. 290022).

References

1. (a) Armand, M.; Endres, F.; MacFarlane, D. R.; Ohno, H.; Scrosati, B., Ionic-liquid materials for the electrochemical challenges of the future. *Nat Mater* **2009,** *8* (8), 621-629; (b) Jeon, S. I.; Lee, J. H.; Andrade, J. D.; De Gennes, P. G., Protein—surface interactions in the presence of polyethylene oxide. *Journal of Colloid and Interface Science* **1991,** *142* (1), 149-158; (c) Lee, J. H.; Lee, H. B.; Andrade, J. D., Blood compatibility of polyethylene oxide surfaces. *Progress in Polymer Science* **1995,** *20* (6), 1043-1079; (d) Desai, N. P.; Hossainy, S. F. A.; Hubbell, J. A., Surface-immobilized polyethylene oxide for bacterial repellence. *Biomaterials* **1992,** *13* (7), 417-420; (e) Fuertges, F.; Abuchowski, A., The clinical efficacy of poly(ethylene glycol)-modified proteins. *Journal of Controlled Release* **1990,** *11* (1–3), 139-148.

2. (a) Lisowski, M. S.; Liu, Q.; Cho, J.; Runt, J.; Yeh, F.; Hsiao, B. S., Crystallization behavior of poly (ethylene oxide) and its blends using time-resolved wide-and small-angle X-ray scattering. *Macromolecules* **2000,** *33* (13), 4842-4849; (b) Huang, C.-I.; Chen, J.-R., Crystallization and chain conformation of semicrystalline and amorphous polymer blends studied by wide-angle and small-angle scattering. *Journal of Polymer Science Part B: Polymer Physics* **2001,** *39* (21), 2705-2715.
3. (a) Schönherr, H.; Frank, C. W., Ultrathin films of poly (ethylene oxides) on oxidized silicon. 2. In situ study of crystallization and melting by hot stage AFM. *Macromolecules* **2003,** *36* (4), 1199-1208; (b) Hobbs, J. K.; Vasilev, C.; Humphris, A. D., Real time observation of crystallization in polyethylene oxide with video rate atomic force microscopy. *Polymer* **2005,** *46* (23), 10226-10236.
4. (a) Massa, M.; Carvalho, J.; Dalnoki-Veress, K., Direct visualisation of homogeneous and heterogeneous crystallisation in an ensemble of confined domains of poly (ethylene oxide). *The European Physical Journal E* **2003,** *12* (1), 111-117; (b) Massa, M. V.; Dalnoki-Veress, K.; Forrest, J., Crystallization kinetics and crystal morphology in thin poly (ethylene oxide) films. *The European Physical Journal E* **2003,** *11* (2), 191-198.
5. Schönherr, H.; Frank, C. W., Ultrathin Films of Poly(ethylene oxides) on Oxidized Silicon. 1. Spectroscopic Characterization of Film Structure and Crystallization Kinetics. *Macromolecules* **2003,** *36* (4), 1188-1198.
6. (a) Meyerhofer, D., *Characteristics of resist films produced by spinning*. AIP: 1978; Vol. 49, p 3993-3997; (b) Emslie, A. G.; Bonner, F. T.; Peck, L. G., FLOW OF A VISCOUS LIQUID ON A ROTATING DISK. *Journal of Applied Physics* **1958,** *29* (5), 858-862.
7. Birnie, D., III; Hau, S.; Kamber, D.; Kaz, D., Effect of ramping-up rate on film thickness for spin-on processing. *Journal of Materials Science: Materials in Electronics* **2005,** *16* (11-12), 715-720.
8. Birnie, D. P., Rational solvent selection strategies to combat striation formation during spin coating of thin films. *Journal of Materials Research* **2001,** *16* (4), 1145-1154.
9. (a) Walheim, S.; Boltau, M.; Steiner, U.; Krausch, G., *Phase separation in thin films of strongly incompatible polymer blends*. 1999; p 75-99; (b) Dalnoki-Veress, K.; Forrest, J. A.; Stevens, J. R.; Dutcher, J. R., Phase separation morphology of spin-coated polymer blend thin films. *Physica A: Statistical Mechanics and its Applications* **1997,** *239* (1-3), 87-94; (c) Dalnoki-Veress, K.; Forrest, J. A.; Stevens, J. R.; Dutcher, J. R., Phase separation morphology of thin films of polystyrene/polyisoprene blends. *Journal of Polymer Science Part B: Polymer Physics* **1996,** *34* (17), 3017-3024.
10. Mellbring, O.; Oiseth, S. K.; Krozer, A.; Lausmaa, J.; Hjertberg, T., Spin coating and characterization of thin high-density polyethylene films. *Macromolecules* **2001,** *34* (21), 7496-7503.
11. (a) Xue, B. F.; Vaughan, B.; Poh, C. H.; Burke, K. B.; Thomsen, L.; Stapleton, A.; Zhou, X. J.; Bryant, G. W.; Belcher, W.; Dastoor, P. C., Vertical Stratification and Interfacial Structure in P3HT:PCBM Organic Solar Cells. *J Phys Chem C* **2010,** *114* (37), 15797-15805; (b) Mokarian-Tabari, P.; Geoghegan, M.; Howse, J. R.; Heriot, S. Y.; Thompson, R. L.; Jones, R. A. L., Quantitative evaluation of evaporation rate during spin-coating of polymer blend films: Control of film structure through defined-atmosphere solvent-casting. *European Physical Journal E* **2010,** *33* (4),

283-289; (c) Dunbar, A. D.; Mokarian-Tabari, P.; Parnell, A. J.; Martin, S. J.; Skoda, M. W.; Jones, R. A., A solution concentration dependent transition from self-stratification to lateral phase separation in spin-cast PS:d-PMMA thin films. *The European physical journal. E, Soft matter* **2010,** *31* (4), 369-75; (d) Heriot, S. Y.; Jones, R. A. L., An interfacial instability in a transient wetting layer leads to lateral phase separation in thin spin-cast polymer-blend films. *Nat Mater* **2005,** *4* (10), 782-786.
12. Takahashi, Y.; Tadokoro, H., Structural Studies of Polyethers, (-(CH2)m-O-)n. X. Crystal Structure of Poly(ethylene oxide). *Macromolecules* **1973,** *6* (5), 672-675.
13. French, A. C.; Thompson, A. L.; Davis, B. G., High-Purity Discrete PEG-Oligomer Crystals Allow Structural Insight. *Angewandte Chemie International Edition* **2009,** *48* (7), 1248-1252.
14. (a) Hammouda, B.; Ho, D. L.; Kline, S., Insight into clustering in poly(ethylene oxide) solutions. *Macromolecules* **2004,** *37* (18), 6932-6937; (b) He, Y.; Zhu, B.; Inoue, Y., Hydrogen bonds in polymer blends. *Progress in Polymer Science* **2004,** *29* (10), 1021-1051; (c) Ho, D. L.; Hammouda, B.; Kline, S. R.; Chen, W. R., Unusual phase behavior in mixtures of poly (ethylene oxide) and ethyl alcohol. *Journal of Polymer Science Part B: Polymer Physics* **2006,** *44* (3), 557-564; (d) Hammouda, B., Clustering in polar media. *The Journal of chemical physics* **2010,** *133* (8), 084901; (e) Polverari, M.; van de Ven, T. G. M., Dilute Aqueous Poly(ethylene oxide) Solutions: Clusters and Single Molecules in Thermodynamic Equilibrium. *The Journal of Physical Chemistry* **1996,** *100* (32), 13687-13695; (f) Kinugasa, S.; Nakahara, H.; Fudagawa, N.; Koga, Y., Aggregative Behavior of Poly(ethylene oxide) in Water and Methanol. *Macromolecules* **1994,** *27* (23), 6889-6892; (g) Faraone, A.; Magazù, S.; Maisano, G.; Migliardo, P.; Tettamanti, E.; Villari, V., The puzzle of poly(ethylene oxide) aggregation in water: Experimental findings. *The Journal of Chemical Physics* **1999,** *110* (3), 1801-1806; (h) Duval, M., Monitoring of Cluster Formation and Elimination in PEO Solutions. *Macromolecules* **2000,** *33* (21), 7862-7867; (i) Polik, W. F.; Burchard, W., Static light scattering from aqueous poly (ethylene oxide) solutions in the temperature range 20-90 C. *Macromolecules* **1983,** *16* (6), 978-982; (j) Zhou, P.; Brown, W., Static and dynamic properties of poly(ethylene oxide) in methanol. *Macromolecules* **1990,** *23* (4), 1131-1139.
15. Polik, W. F.; Burchard, W., Static light scattering from aqueous poly(ethylene oxide) solutions in the temperature range 20-90°C. *Macromolecules* **1983,** *16* (6), 978-982.
16. (a) Halls, J. J. M.; Arias, A. C.; MacKenzie, J. D.; Wu, W.; Inbasekaran, M.; Woo, E. P.; Friend, R. H., Photodiodes based on polyfluorene composites: influence of morphology. *Adv. Mater. (Weinheim, Ger.)* **2000,** *12* (Copyright (C) 2012 American Chemical Society (ACS). All Rights Reserved.), 498-502; (b) Arias, A. C.; MacKenzie, J. D.; Stevenson, R.; Halls, J. J. M.; Inbasekaran, M.; Woo, E. P.; Richards, D.; Friend, R. H., Photovoltaic Performance and Morphology of Polyfluorene Blends: A Combined Microscopic and Photovoltaic Investigation. *Macromolecules* **2001,** *34* (17), 6005-6013; (c) Brabec, C. J.; Durrant, J. R., Solution-processed organic solar cells. *Mrs Bulletin* **2008,** *33* (7), 670-675; (d) Brabec, C. J.; Heeney, M.; McCulloch, I.; Nelson, J., Influence of blend microstructure on bulk heterojunction organic photovoltaic performance. *Chemical Society Reviews* **2011,** *40* (3), 1185-1199; (e) Schuettfort, T.; Watts, B.;

Thomsen, L.; Lee, M.; Sirringhaus, H.; McNeill, C. R., Microstructure of Polycrystalline PBTTT Films: Domain Mapping and Structure Formation. *Acs Nano* **2012,** *6* (2), 1849-1864; (f) Aylott, J. W.; Richardson, D. J.; Russell, D. A., Optical biosensing of gaseous nitric oxide using spin-coated sol-gel thin films. *Chemistry of Materials* **1997,** *9* (11), 2261-2263.
17. (a) Chou, K. W.; Yan, B.; Li, R.; Li, E. Q.; Zhao, K.; Anjum, D. H.; Alvarez, S.; Gassaway, R.; Biocca, A.; Thoroddsen, S. T.; Hexemer, A.; Amassian, A., Spin-cast bulk heterojunction solar cells: a dynamical investigation. *Adv Mater* **2013,** *25* (13), 1923-9; (b) Perez, L. A.; Chou, K. W.; Love, J. A.; van der Poll, T. S.; Smilgies, D.-M.; Nguyen, T.-Q.; Kramer, E. J.; Amassian, A.; Bazan, G. C., Solvent Additive Effects on Small Molecule Crystallization in Bulk Heterojunction Solar Cells Probed During Spin Casting. *Advanced Materials* **2013,** *25* (44), 6380-6384.
18. Toolan, D. T. W.; Howse, J. R., Development of in situ studies of spin coated polymer films. *Journal of Materials Chemistry C* **2013,** *1* (4), 603-616.
19. (a) Jukes, P. C.; Heriot, S. Y.; Sharp, J. S.; Jones, R. A. L., Time-Resolved Light Scattering Studies of Phase Separation in Thin Film Semiconducting Polymer Blends during Spin-Coating. *Macromolecules* **2005,** *38* (6), 2030-2032; (b) Toolan, D. T. W.; Haq, E. u.; Dunbar, A.; Ebbens, S.; Clarke, N.; Topham, P. D.; Howse, J. R., Direct observation of morphological development during the spin-coating of polystyrene-poly(methyl methacrylate) polymer blends. *Journal of Polymer Science Part B: Polymer Physics* **2013,** *51* (11), 875-881; (c) Toolan, D. T. W.; Parnell, A. J.; Topham, P. D.; Howse, J. R., Directed phase separation of PFO:PS blends during spin-coating using feedback controlled in situ stroboscopic fluorescence microscopy. *Journal of Materials Chemistry A* **2013,** *1* (11), 3587-3592; (d) Toolan, D. T. W.; Hodgkinson, R.; Howse, J. R., Stroboscopic Microscopy-Direct Imaging of Structure Development and Phase Separation During Spin-Coating. *Journal of Polymer Science Part B-Polymer Physics* **2014,** *52* (1), 17-25.
20. (a) Toolan, D. T.; Pullan, N.; Harvey, M. J.; Topham, P. D.; Howse, J. R., In situ studies of phase separation and crystallization directed by Marangoni instabilities during spin-coating. *Adv Mater* **2013,** *25* (48), 7033-7; (b) Toolan, D. T., Straightforward technique for in situ imaging of spin-coated thin films. *Optical Engineering* **2015,** *54* (2), 024109-024109.
21. Toolan, D. T. W.; Pullan, N.; Harvey, M. J.; Topham, P. D.; Howse, J. R., In Situ Studies of Phase Separation and Crystallization Directed by Marangoni Instabilities During Spin-Coating. *Advanced Materials* **2013,** *25* (48), 7033-7037.
22. Brandrup, J.; Immergut, E. H.; Grulke, E. A.; Abe, A.; Bloch, D. R., *Polymer handbook*. Wiley New York: 1999; Vol. 89.
23. Özdemir, C.; Güner, A., Solubility profiles of poly(ethylene glycol)/solvent systems, I: Qualitative comparison of solubility parameter approaches. *European Polymer Journal* **2007,** *43* (7), 3068-3093.
24. (a) Van Antwerpen, F.; Van Krevelen, D., Influence of crystallization temperature, molecular weight, and additives on the crystallization kinetics of poly (ethylene terephthalate). *Journal of Polymer Science: Polymer Physics Edition* **1972,** *10* (12), 2423-2435; (b) Machado, J. C.; Silva, G. G.; Oliveira, F. C. d.; Lavall, R. L.; Rieumont, J.; Licinio, P.; Windmöller, D., Free-volume and crystallinity in low molecular weight poly(ethylene oxide). *Journal of Polymer Science Part B: Polymer Physics* **2007,** *45* (17), 2400-2409.
25. Wang, T.; Dunbar, A. D. F.; Staniec, P. A.; Pearson, A. J.; Hopkinson, P. E.; MacDonald, J. E.; Lilliu, S.; Pizzey, C.; Terrill, N. J.; Donald, A. M.; Ryan, A. J.; Jones,

R. A. L.; Lidzey, D. G., The development of nanoscale morphology in polymer:fullerene photovoltaic blends during solvent casting. *Soft Matter* **2010,** *6* (Copyright (C) 2011 American Chemical Society (ACS). All Rights Reserved.), 4128-4134.
26. (a) Kolmogorov, A. N., On the statistical theory of the crystallization of metals. *Bull. Acad. Sci. USSR, Math. Ser* **1937,** *1*, 355-359; (b) Johnson, W. A.; Mehl, R. F., Reaction kinetics in processes of nucleation and growth. *Trans. Aime* **1939,** *135* (8), 396-415; (c) Avrami, M., Kinetics of phase change. II transformation - time relations for random distribution of nuclei. *The Journal of Chemical Physics* **1940,** *8* (2), 212-224.
27. Birnie, D. P.; Zelinski, B. J. J.; Perry, D. L., INFRARED OBSERVATION OF EVAPORATIVE COOLING DURING SPIN-COATING PROCESSES. *Optical Engineering* **1995,** *34* (6), 1782-1788.
28. Heeley, E. L.; Maidens, A. V.; Olmsted, P. D.; Bras, W.; Dolbnya, I. P.; Fairclough, J. P. A.; Terrill, N. J.; Ryan, A. J., Early Stages of Crystallization in Isotactic Polypropylene. *Macromolecules* **2003,** *36* (10), 3656-3665.

For table of contents only

Insights into the influence of solvent polarity on the crystallization of poly(ethylene oxide) spin-coated thin films via *in situ* grazing incidence wide angle x-ray scattering.

Daniel T. W. Toolan,[1] Anna Isakova,[2] Richard Hodgkinson,[1] Nik Reeves-McLaren,[3] Oliver S. Hammond,[4] Karen J. Edler,[4] Wuge H. Briscoe,[5] Thomas Arnold,[6] Tim Gough,[7] Paul D. Topham,[2] and Jonathan R. Howse.[1*]